# Chirality and fermions

*Gerhard H. Fecher[#], Kaustuv Manna[##], Walter Schnelle[###], Yan Sun[####], Claudia Felser[#####]*

**Chirality is related to special symmetry. For crystal structures, it describes the absence of mirror planes and inversion centers and, besides translations, only rotations are allowed. We investigated various compounds with the chiral B20 (FeSi) structure. One aim was to determine the signatures of exotic fermions, such as 4-fold spin S = 3/2 crossing, denoted the Rarita-Schwinger fermion, at the Γ point and 6-fold S = 1 crossing at the R point of the Brillouin zone, forming a novel type of fermionic excitation within the electronic structures of chiral compounds. Of these exotic fermions, the massive Dirac fermions are helical and the massless Weyl fermions are chiral with the maximal Chern number ±4.**

Chirality characterizes special, symmetry-dependent properties of matter. In the field of chemistry, the main focus is on molecular chirality, but crystal and surface chirality is also critical. According to Lord Kelvin, chirality is the absence of mirror planes and inversion centers, i.e. it describes objects that cannot be superimposed on their mirror images. Chiral solids are classified by the 65 Sohnke groups, of which 22 are chiral. In addition, magnetic systems may exhibit spin-chirality, which describes the symmetries of the magnetic moments in solids with noncollinear spin order, including spin glasses. The vector spin-chirality is related to the antisymmetric exchange interaction, also known as the Dzyaloshinskii–Moriya interaction.

Crystal structure chirality may be quantified using the chirality measure: $s^2 = \sum ||p_i - p_i^{\mathrm{sym}}||^2$ , where $p_i$ are the points of the actual structure and $p^{\mathrm{sym}}$ are those of the closest achiral structure. The latter may be a rock-salt or zinc-blende structure, depending on the actual position parameters *u*.

In the field of particle physics, chirality describes a relativistic quantum mechanical state. In particular, helicity and chirality are not always the same. Helicity is defined by the projection of the spin onto the direction of linear momentum, whereas chirality is a property of the relativistic Hamiltonian and, in particular, of spinors. For massless particles that move at the speed of light, helicity and chirality are the same. For massive particles, the helicity depends on the velocity of the particle relative to the observer. Their quantum mechanical state is thus a mixture of two opposing chiralities. Dirac fermions are massive and thus helical, whereas Weyl fermions are massless and thus chiral.

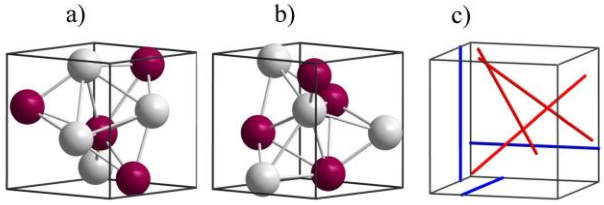


*Fig. 1: Representative crystal structure of the B20 compounds. (a) and (b) show an enantiomorphous pair of structures (u parameters for PdGa). In (c), the 2- and 3-fold screw axes are shown in blue and red, respectively. Applying the $2_1$ screw rotations to the atoms at (u,u,u) generates the other 3 atom positions of each substructure.*

The B20 structure is a simple, chiral, cubic crystal structure that belongs to the space group $P2_13$ (no. 198). The prototype is FeSi and approximately 30 compounds containing one transition metal and one main group element crystallize in this structure. The space group contains 12 symmetry elements: the unity operator, three 2-fold and three 3-fold screw axes, and five regular, simple 3-fold rotational axes. An example of the latter is a 3-fold rotation about the [111] axis. The three $2_1$ screw axes are parallel to the principle axes along the lines [1/4,0,*z*], [0,*y*,1/4], and [*x*,1/4,0]. The three $3_2$ screw axes are along the lines [*x*+1/6, -*x*+1/6,-*x*], [-*x*+1/3,-*x*+1/6,*x*], and [-*x*-1/6,*x*+1/3,-*x*]. The crystal structure and screw axes are displayed in Fig. 1. Both atoms are placed at Wyckoff positions 4a (*u*,*u*,*u*). The structure consists of two enantiomeric substructures. The substructure with 0<*u*<¼ or ½<*u*< ¾ is left chiral and the one with ¼< *u*<½ or ¾< *u*<1is right chiral. At *u* = 0, ¼, ½, or ¾ the structure is achiral.

Several compounds with B20 structure are investigated with respect to different physical aspects: CoSi [1, 2], PdGa [3, 4], PtAl [5], PtGa [6], and RhSi [1, 7–9]. Table 1 summarizes their structural parameters $u_i$ and chirality measures.

*Table 1: Structural parameters of B20 compounds*

| | $u_{\mathrm{TM}}$ | $u_{\mathrm{MG}}$ | $S^2$ (%) |
|---|---|---|---|
| CoSi | 0.395 | 0.094 | 62.9 |
| PdGa | 0.393 | 0.093 | 64.5 |
| PtAl | 0.404 | 0.094 | 57.6 |
| PtGa | 0.398 | 0.093 | 61.0 |
| RhSi | 0.402 | 0.092 | 57.9 |

**Properties of chiral B20 compounds**

The first observation of the topological quantum properties of chiral crystals using angular-resolved photoelectron spectroscopy (ARPES) was reported for CoSi and RhSi by Sanchez et al. [1]. Almost ideal topological surface properties were detected, originating from the crystal structure chirality. Electrons on the crystal surfaces exhibited a highly unusual helicoid fermionic structure that spiraled around two high-symmetry momenta, indicating electronic topological chirality. The helicoid arcs observed on the crystal surfaces suggested topological charges of ±2 arising from bulk higher-spin chiral fermions.

The ab initio calculations of the electronic structures of CoSi and RhSi are shown in Fig. 2a together with an illustration of the Brillouin zone with its irreducible edge in Fig. 2b. The bulk band structures indicate – independent of their handedness − that the chiral crystals exhibit a 3-fold degeneracy at Γ near the Fermi energy $E_F$. $E_F$ is described by a low energy Hamiltonian that exhibits a 3-fold fermion associated with Chern number +2. This Chern number is referred to as chiral charge − a usage of the term *'chiral'* that is distinct from structural chirality and motivates the use of the term *'chiral fermion'* to describe these topological band crossings. The R point hosts a 4-fold degeneracy corresponding to a 4-fold fermion with Chern number −2. These two higher-fold chiral fermions are pinned to opposing time-reversal-invariant momenta and are consequently constrained to be maximally separated in momentum space (see Fig. 1b). CoSi and RhSi possess only two chiral fermions in the bulk BZ, the minimum non-zero number allowed, and thus, they satisfy a key criterion for an ideal topological conductor. As shown in Fig 1a, CoSi maintains constant-energy surfaces with a non-zero Chern number over an energy window of 0.85 eV, whereas for RhSi, this window is 1.3 eV. The calculated Fermi surface (Fig. 1c) shows that the projection of the higher-fold chiral fermions to the (0 0 1) surface results in a hole (electron) pocket at Γ(M) with Chern number ±2. The topological properties of CoSi were more closely examined by investigating the structures of the Fermi arcs near M (see the dispersion on P, plotted as a magenta loop in Fig. 3a).

The observed decrease in the binding energy (approaching $E_F$) and the extracted clockwise dispersion spirals of both loops suggest that as a given point *k* traverses the loop, the energy of the state does not return to its initial value after a full cycle. This non-trivial electronic dispersion directly signals a projected chiral charge at M (Fig. 3a). Moreover, the extracted dispersion is characteristic of the helicoid structures of

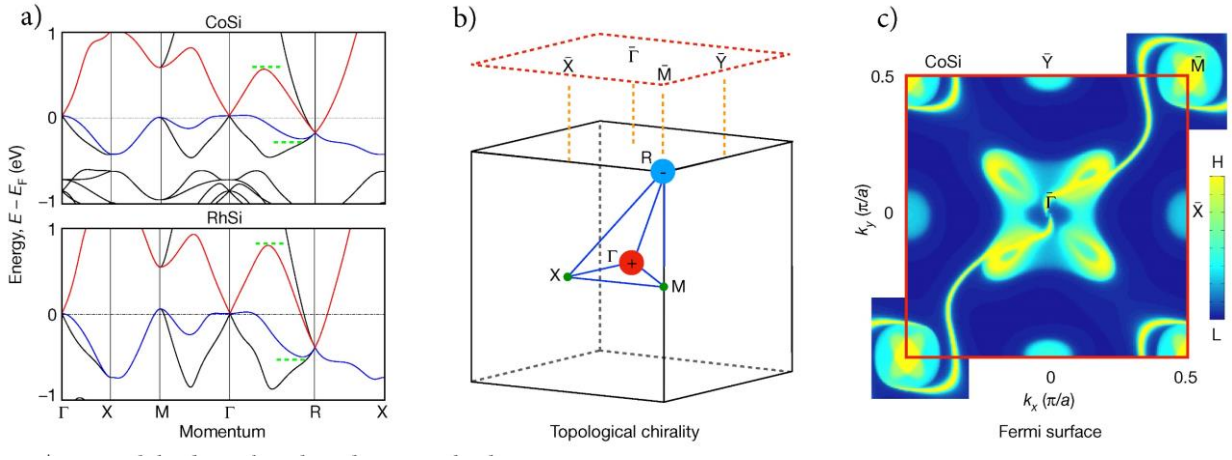


*Fig. 2: Topological quantum chiralities in CoSi and RhSi*

*a) Ab initio calculation of the electronic bulk band structure along high-symmetry lines. A 3-fold-degenerate topological chiral fermion is predicted at Γ and a 4-fold topological chiral fermion is predicted at R, with Chern numbers +2 and −2, respectively. The highest valence (blue) and lowest conduction (red) bands indicate a topologically non-trivial energy window (green dashed lines).*

*b) Bulk BZ and (0 0 1) surface BZ with high-symmetry points; the predicted chiral fermions (red and blue spheres) are labelled.*

*c) Ab initio calculation of the surface spectral weight on the (0 0 1) surface for CoSi, with the (0 0 1) surface BZ indicated (red box). The predicted bulk chiral fermions project onto Γ and M, connected by a pair of topological Fermi arcs extending diagonally across the surface BZ. The color bar limits correspond to high (H) and low (L) electron density.*

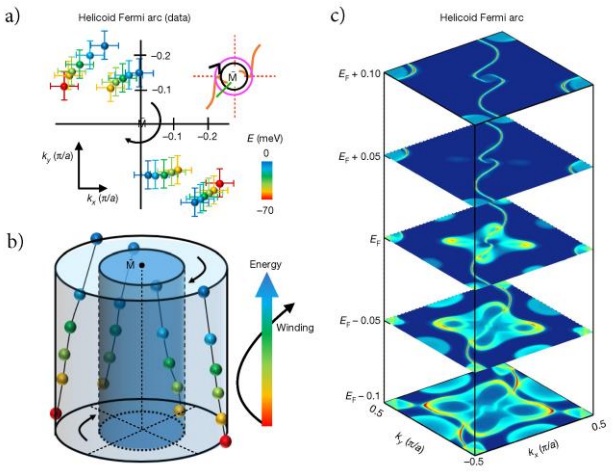


*Fig. 3: Helicoid quantum arcs in CoSi.*

- *a) From angular-resolved photoelectron spectroscopy (ARPES), we extracted the dispersion of the chiral edge modes on P and a second inner loop from a Lorentzian fit.*
- *b) Perspective plot of a), with the two loops shown as two concentric cylinders. The winding of the chiral modes around M as a function of the binding energy suggests that the Fermi arcs have a helicoid structure.*
- *c) Calculated constant-energy contours that are consistent with the helicoid Fermi arc structure observed in the spectra.*

topological Fermi arcs as they wind around a chiral fermion (Fig. 3b), suggesting that CoSi and RhSi are rare examples of non-compact surfaces. Fig. 3c shows a pair of Fermi arcs winding around the Γ and M pockets counterclockwise and clockwise, respectively, with decreasing binding energy when approaching $E_F$.

The topological charges of CoSi and RhSi determined using ARPES were both ±2, in contrast with the original prediction of Chern number ±4 for the two multifold Weyl points at the high symmetric momenta at the Γ and R points. Due to the low spin-orbit coupling, the Fermi arc splitting was beyond the experimental resolution. Therefore, PtGa, PdGa, and PtAl were examined.

Schröter et al. [5] showed that PtAl was also a structurally chiral topological semimetal that hosted 4- and 6-fold fermions, which were viewed as a higher-spin generalization of Weyl fermions without equivalence in the field of elementary particle physics. These multifold fermions were located at high-symmetry points with Chern numbers larger than those in conventional non-chiral Weyl semimetals, thus resulting in multiple Fermi arcs spanning the full diagonal of the surface Brillouin zone.

Based on the large *Z* of Pt, PtGa [6] exhibited the strongest spin-orbit interaction among the investigated chiral crystals. High-resolution ARPES (https://www1.cpfs.mpg.de:2443/SSC_06) and ab initio calculations revealed a large spin-orbit splitting of the Fermi arcs and bulk states. This confirmed the maximal Chern number ±4 associated with the multifold fermions at the Γ and R points of these chiral topological semimetals.

To investigate how to control and tune the topological states, detailed ARPES and scanning tunneling microscopy (STM) studies were conducted on enantiomorphous PdGa single crystals [3, 4]. Multifold band crossings were observed, which were connected by exactly 4 surface Fermi arcs, thus establishing that they had the maximal Chern number magnitude of 4. By comparing two enantiomers, a reversal of their Fermi arc velocities was observed, which demonstrated that the chirality was used to control the signs of the Chern numbers. A direct manifestation of the sign change of the Chern number was revealed from chiral quantum interference patterns of opposite spiraling directions for the PdGa enantiomers, observed using STM.

The multifold band crossing with the maximal Chern number ±4 promised several favorable phenomena, including chiral magnetic effects, highly efficient catalyzes, and large quantized photoresponses to circularly polarized light. Using first-principle calculations, the optical conductivities above and below 0.2 eV were linked to interband transitions near double Weyl and 3-fold fermions, respectively [2]. At energies below 0.1 eV, the optical response was governed by transitions between a previously unobserved 4-fold spin-3/2 node and a Weyl node.

Optical conductivity was measured for RhSi to investigate its multifold fermions [7]. The linear behavior of the interband conductivity was related to transitions between the linear bands near the band crossing points. Associated with each crossing point (or Weyl node) was a topological invariant denoted as the Berry monopole charge, manifesting as a circular photogalvanic effect, whereby circularly polarized light generated a helicity-dependent photo-current [8, 9].

**Future prospects**

A future challenge is to synthesize more enantio-morphous pairs of crystals from different compounds for detailed electronic structure comparisons. Compounds with other chiral structures, aside from the

B20 compounds, should be synthesized, particularly those with chiral structures and accompanying chiral space groups (e.g. low quartz that crystallizes in the chiral space groups $P4_12_12$ (94) or $P4_32_12$ (96)). A closer association between structural and fermion chirality requires additional investigation, e.g. using circular dichroism.

The electronic structure is mainly investigated using ARPES to study the surfaces, resulting in a further challenge. Due to the lack of mirror and inversion symmetries, the opposite surfaces of a chiral crystal are non-equivalent. For example, the (0 0 1) and (0 0 –1) surfaces of the B20 structure are largely different. A complete determination and characterization of the chirality or handedness of the electronic structure always requires at least 4 measurements, 2 for the opposite surfaces of an enantiomorphous pair of crystals.

**External Cooperation Partners**

M. Zahid Hasan (Princeton University); Yulin Chen (University of Oxford); Joseph Orenstein (UC Berkeley); Liang Wu (University of Pennsylvania); Niels B. M. Schröter (Max Planck Institute of Microstructure Physics, Halle, Germany).

**References**


[1]* *Topological chiral crystals with helicoid-arc quantum states, D. S. Sanchez, I. Belopolski, T. A. Cochran, X. Xu, J.-X. Yin, G. Chang, W. Xie, K. Manna, V. Süß, C.-Y. Huang, et al., Nature **567** (2019) 500.*

[2]* *Optical signatures of multifold fermions in the chiral topological semimetal CoSi, B. Xu, Z. Fang, M.-A. Sanchez-Martınez, J. W. F. Venderbos, Z. Ni, T. Qiu, K. Manna, K. Wang, J. Paglione, Ch. Bernhard, et al., PNAS **117** (2020) 27104.*

[3]* *Handedness-dependent quasiparticle interference in the two enantiomers of the topological chiral semimetal PdGa, P. Sessi, F.-R. Fan, F. Küster, K. Manna, N. B. M. Schröter, J.-R. Ji, S. Stolz, J. A. Krieger, D. Pei, T. K. Kim, et al., Nature Comm **11** (2020) 3507.*

[4]* *Observation and control of maximal Chern numbers in a chiral topological semimetal, N. B. M. Schröter, S. Stolz, K. Manna, F. de Juan, M. G. Vergniory, J. A. Krieger, D. Pei, T. Schmitt, P. Dudin, T. K. Kim, et al., Science **369** (2020) 179.*

[5]* *Chiral topological semimetal with multifold band crossings and long Fermi arcs, N. B. M. Schröter, D. Pei, M. G. Vergniory, Y. Sun, K. Manna, F. de Juan, J. A. Krieger, V. Süss, M. Schmidt, P. Dudin, et al., Nature Phys **15** (2019) 759.*

[6]* *Observation of giant spin-split Fermi-arc with maximal Chern number in the chiral topological semimetal PtGa, M. Yao, K. Manna, Q. Yang, A. Fedorov, V. Voroshnin, B. V. Schwarze, J. Hornung, S. Chattopadhyay Z. Sun, S. N. Guin, et al., Nature Comm **11** (2020) 2033.*

[7]* *Optical conductivity of multifold fermions: The case of RhSi, L. Z. Maulana, K. Manna, E. Uykur, C. Felser, M. Dressel, and A. V. Pronin, Phys Rev Res **2** (2020) 023018.*

[8]* *Linear and nonlinear optical responses in the chiral multifold semimetal RhSi, Z. Ni, B. Xu, M.-Á. Sánchez-Martínez, Y. Zhang, K. Manna, C. Bernhard, J. W. F. Venderbos, F. de Juan, C. Felser, A. G. Grushin, and L. Wu, npjQuantMats **96** (2020) 1.*

[9]* *Helicity-dependent photocurrents in the chiral Weyl semimetal RhSi, D. Rees, K. Manna, B. Lu, T. Morimoto, H. Borrmann, C. Felser, J. E. Moore, D. H. Torchinsky, and J. Orenstein, Sci Adv **6** (2020) eaba0509.*



# fecher@cpfs.mpg.de
## kaustuvmanna@iitd.ac.in
### schnelle@cpfs.mpg.de
#### ysun@cpfs.mpg.de
##### felser@cpfs.mpg.de